Peptide Probe Study of the Role of Interaction between the Cytoplasmic and Transmembrane Domains of the Ryanodine Receptor in the Channel Regulation Mechanism†

Tomoyo Hamada,‡ Mark L. Bannister,‡ and Noriaki Ikemoto*,‡,§

Boston Biomedical Research Institute, Watertown, Massachusetts 02472, and Department of Neurology, Harvard Medical School, Boston, Massachusetts 02115

Received August 1, 2006; Revised Manuscript Received January 17, 2007

ABSTRACT: Ryanodine receptor (RyR) mutations linked with some congenital skeletal and cardiac diseases are localized to three easily definable regions: region 1 (N-terminal domain), region 2 (central domain), and a rather broad region 3 containing the channel pore. As shown in our recent studies, the interdomain interaction between regions 1 and 2 plays a critical role in channel regulation and pathogenesis. Here we present evidence that within region 3 there is a similar channel regulation mechanism mediated by an interdomain interaction. DP15, a peptide corresponding to RyR1 residues 4820−4841, produced significant activation of [^{3}H]ryanodine binding above threshold Ca^{2+} concentrations (≥ 0.3 μM), but MH mutations (L4823P or L4837V) made in DP15 almost completely abolished its channel activating function. To identify the DP15 binding site(s) within RyR1, DP15 (labeled with a fluorescent probe Alexa Fluor 680 and a photoaffinity cross-linker APG) was cross-linked to RyR1, and the site of cross-linking was identified by gel analysis of fluorescently labeled proteolytic fragments with the aid of Western blotting with site-specific antibodies. The shortest fluorescently labeled band was a 96 kDa fragment which was stained with an antibody directed to the region of residues 4114−4142 of RyR1, indicating that the interaction between the region of residues 4820−4841 adjacent to the channel pore and the 96 kDa segment containing the region of residues 4114−4142 is involved in the mechanism of Ca^{2+}-dependent channel regulation. In further support of this concept, anti-DP15 antibody and cardiac counterpart of DP15 produced channel activation similar to that of DP15.

Skeletal muscle-type e−c coupling[1] is activated by the voltage-mediated interaction of the dihydropyridine (DHP) receptor with RyR1, while in cardiac muscle, the voltage-sensing process is immediately followed by the opening of the DHPR Ca^{2+} channel, causing flux of Ca^{2+} into the cytoplasm, and activation of RyR2. However, little is known about how the activation signal received by the cytoplasmic domain of the RyR is transmitted to the Ca^{2+} channel. In searching for critical domains involved in this intramolecular signal transmission mechanism, we have paid particular attention to the distribution of mutations linked with some skeletal (MH and CCD) and cardiac (CPVT and ARVD2) diseases. As widely recognized, they are localized to three easily definable regions [region 1 (N-terminal domain), region 2 (central domain), and a rather broad region 3 containing the channel pore], suggesting that these three regions represent critical regulatory domains. According to the model deduced from our recent studies (*1*−*4*), the N-terminal and central domains make close contact at several subdomains, forming a pair of interacting domains (designated as a "domain switch"). The conformational constraints imparted by the "zipped" configuration of the two domains stabilize and maintain the closed state of the Ca^{2+} channel. Upon reception of the activation signal, these critical interdomain contacts are weakened (domain unzipping), leading to Ca^{2+} channel opening. Weakening of the interdomain interactions also is caused by mutation in either domain or various agents that cause unzipping between the N-terminal and central domains (e.g., domain peptides and antibodies).

An increasing number of skeletal (MH and CCD) and cardiac (CPVT) mutations has been reported in region 3. George et al. reconstituted the agonist regulation of the channel by coexpressing the transmembrane Ca^{2+} channel pore domain and a panel of cytoplasmic domains of RyR2 in living cells and found that the region of residues 3722−4610 of RyR2 (corresponding to residues 3760−4679 of RyR1), designated as the interaction domain (I domain), may

† This work was supported by National Institutes of Health Grants AR 16922 from the National Institute of Arthritis and Musculoskeletal and Skin Diseases and HL072841 from the National Heart, Lung and Blood Institute.

* To whom correspondence should be addressed: Boston Biomedical Research Institute, 64 Grove St., Watertown, MA 02472. Telephone: (617)658-7774. Fax: (617)972-1761. E-mail: ikemoto@bbri.org.

‡ Boston Biomedical Research Institute.

§ Harvard Medical School.

[1] Abbreviations: APG, *p*-azidophenyl glyoxal monohydrate; ARVD2, arrhythmogenic right ventricular cardiomyopathy; BAPTA, 1,2-bis(*o*-aminophenoxy)ethane-*N*,*N*,*N*′,*N*′-tetraacetic acid; CaM, calmodulin; CaMBP, calmodulin binding region peptide; CCD, central core disease; CPVT, catecholaminergic polymorphic ventricular tachycardia; DHP, dihydropyridine; DTT, 1,4-dithiothreitol; e−c coupling, excitation−contraction coupling; MH, malignant hyperthermia; RyR, ryanodine receptor; SR, sarcoplasmic reticulum.

10.1021/bi061557f CCC: $37.00
Published on Web 03/16/2007

be involved in the interaction between the regulatory cytoplasmic domain and the transmembrane channel domain (*5*). This suggests that interdomain interactions within region 3 may play a critical role in channel regulation and pathogenesis. Furthermore, the recent finding by Gilman et al. that peptides matching the N-terminal and C-terminal segments of region 3 bound with each other also suggests an interdomain interaction within region 3 (*6*). We here present evidence that the interaction between the region of residues 4820−4841 (one of the cytoplasmic loops of the transmembrane channel domain) and a 96 kDa segment containing the region of residues 4114−4142 plays a key role in the regulation of RyR1 channels and pathogenesis.

EXPERIMENTAL PROCEDURES

Materials. Reagents and chemicals were obtained from Fisher, Invitrogen, or Sigma unless otherwise stated.

Preparation of SR Vesicles. SR vesicles were prepared from rabbit back paraspinous and hind leg skeletal muscle (Pel-Freez Biologicals) using differential centrifugation (*7*). Microsomes from the final centrifugation were homogenized in 0.3 M sucrose, 0.15 M KCl, proteolytic enzyme inhibitors (0.1 mM phenylmethanesulfonyl fluoride, 1 μg/mL leupeptin, and 2 μg/mL soybean trypsin inhibitor), and 20 mM MES (pH 6.8) to a final concentration of 15−30 mg/mL, frozen immediately in liquid N_2, and stored at −80 °C.

Domain Peptides Synthesis. The peptides were synthesized on an Applied Biosystems model 431A synthesizer, purified by reversed-phase high-pressure liquid chromatography, and evaluated by mass spectroscopy. Domain peptides based on sections of region 3 of rabbit RyR1 are as follows: DP15 (residues 4820−4841), DP17 (residues 4114−4142), DP19 (residues 4726−4754), and DP18 (residues 4223−4259). DPc15 corresponds to residues 4752−4773 of rabbit RyR2. DP15mut (L4823P) and DP15mut (L4837V) contain the L4824P and L4838V mutations of human RyR1, respectively (*8*−*11*), and DPc15mut (H4764P) contains the H4762P mutation of human RyR2 (*12*). DP17mut (R4137S) contains the R4136S mutation of human RyR1 (*13*).

[^{3}H]Ryanodine Binding Assay. SR vesicles (0.5 mg/mL) were incubated in a solution containing 10 nM [^{3}H]ryanodine (50−100 Ci/mmol, Perkin-Elmer Life Sciences), 0.15 M KCl, 2 mM DTT, 20 mM MOPS (pH 7.2), and various concentrations of free Ca^{2+} at 37 °C for 2 h, in the absence or presence of domain peptides in a final volume of 0.1 mL. For DP17 and antibody experiments, 2 mM DTT was omitted from solutions. The incubation for antibody experiments was performed at 22 °C overnight. The concentration of free Ca^{2+} was adjusted with BAPTA/calcium buffers; the free Ca^{2+} concentration was calculated from the concentration of BAPTA (Molecular Probes) added and the total amount of calcium in the solution (added $CaCl_2$). Samples were filtered onto glass fiber filters (Whatman GF/B) and washed three times with 2.5 mL (in each washing step) of distilled water. The filters were then placed in scintillation vials containing 4 mL of Ecoscint A scintillation mixture and counted in a Beckman LS 3801 counter. The extent of specific binding was calculated as the difference between the binding in the absence (total binding) and presence (nonspecific binding) of 20 μM nonradioactive ryanodine. The assays were carried out in duplicate, and each datum point was obtained by averaging the duplicates (three to nine experiments).

Alexa Fluor 680 Labeling of the DP15 Binding Region. Fluorescent labeling of DP15 was performed by using the protocol of Alexa Fluor conjugation (Molecular Probes). The Alexa Fluor 680−DP15 conjugate was formed by incubating 0.25 mM DP15 with 0.25 mM Alexa Fluor 680 carboxylic acid, succinimidyl ester in 20 mM HEPES (pH 7.5) at 22 °C for 1 h in the dark. *p*-Azidophenyl glyoxal monohydrate (APG) (Pierce), an arginine-specific cross-linker bearing a photoreactive group, was added to a final concentration of 0.5 mM and the mixture incubated at 22 °C for 1 h in the dark. The reaction was stopped with 20 mM lysine and arginine. The conjugate was purified with spin columns of Sephadex G-15 to remove the free reactants. The Alexa Fluor 680−DP15−APG conjugate (final concentration of 5 μM) was mixed with 2 mg/mL SR in 0.15 M KCl and 20 mM MOPS (pH 7.2) containing 1 mM BAPTA and 1.01 mM $CaCl_2$ (10 μM free Ca^{2+}) in the dark and photolyzed with UV light in a Pyrex tube for 1 min. The mixture was centrifuged at 14000*g* for 5 min, and the pellet was resuspended with 0.15 M NaCl and 20 mM MOPS (pH7.2) after being washed with buffer. For calpain digestion, the samples were incubated with 0.02 unit/μL calpain II (Calbiochem) and 3 mM $CaCl_2$ for 15 min at 22 °C, and the reaction was stopped with 3 mM BAPTA. After calpain digestion, various concentrations of trypsin [SR:trypsin (w:w) ratios of 40000:1, 16000:1, 8000:1, 4000:1, and 1000:1] were added and the mixtures incubated at 22 °C for 20 min, and the reaction was stopped with 1 mg/mL trypsin inhibitor. The sample was centrifuged at 14000*g* for 5 min to remove the solution and mixed with the SDS sample buffer. SDS−PAGE was performed as described by Laemmli (*14*). The fluorescence image of the gel was obtained with an Odyssey infrared image scanner (LI-COR).

Antibody Preparation and Western Blotting. The rabbit antisera against DP15 and DP17 were raised by Bio-Synthesis. Antibodies for CaMBP, DP15, and DP17 were purified with domain peptide-bound affinity columns (Pierce), and concentrations were determined as described previously (*4*). A Western blot was performed using the protocol of the ECL Western Blotting System (Amersham Biosciences). Antidomain peptide antibodies (anti-CaMBP, 1:10000; and anti-DP17, 1:1000) were used for the primary antibody, and horseradish peroxidase-conjugated anti-rabbit IgG antibody (1:50000) (Pierce) was used for the secondary antibody.

Statistical Analysis. Results are expressed as means ± the standard error of the mean. The significance of the mean values was shown as the *P* value calculated with Student's *t* tests.

RESULTS

Domain Peptide DP15 Activates RyR1 at High Ca^{2+} Concentrations. We tested four domain peptides based on subdomains of region 3 of RyR1 containing mutable residues: DP17 (residues 4114−4142), DP18 (residues 4223−4259), DP19 (residues 4726−4754), and DP15 (residues 4820−4841). Three of the four (DP17, DP19, and DP15) produced appreciable activation on RyR1 channels as determined with a ryanodine binding assay (data not shown for DP19). DP15, which matches the region of residues 4820−4841, the cytoplasmic loop between TM6 and TM7 (*15*, *16*; also see Figure 8), produced the most

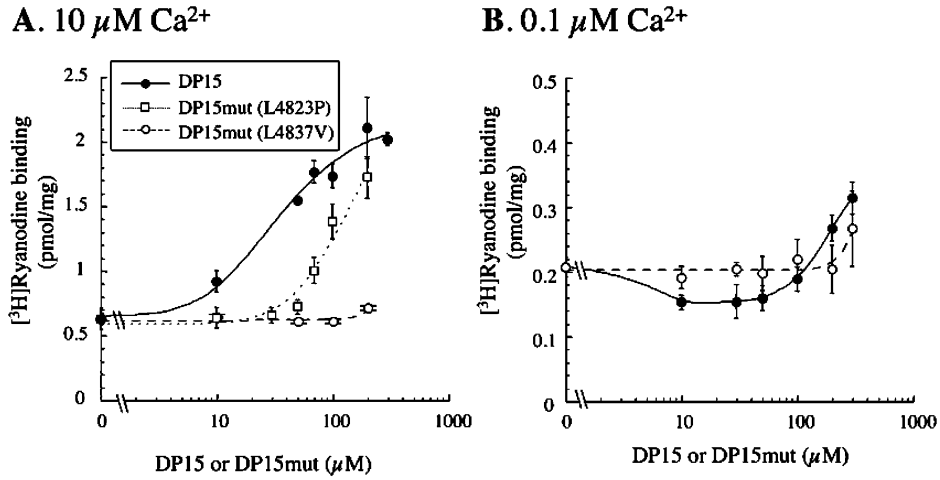

FIGURE 1: Concentration dependence of DP15 and DP15mut on binding of [^{3}H]ryanodine to RyR1. (A) Rabbit skeletal SR (0.5 mg/mL) was incubated with 10 nM [^{3}H]ryanodine in a solution of 0.15 M KCl, 20 mM MOPS (pH 7.2), 2 mM DTT, and various concentrations of DP15 (●), DP15mut (L4823P) (□), and DP15mut (L4837V) (○) at 10 μM Ca^{2+}. $n = 4-9$ for DP15, and $n = 3-4$ for DP15mut. (B) Similar experiments were performed at 0.1 μM Ca^{2+}. $n = 3-6$ for DP15, and $n = 3-6$ for DP15mut.

pronounced effect. At 10 μM Ca^{2+}, DP15 activated [^{3}H]-ryanodine binding with an EC_{50} of ~30 μM, and at maximally activating concentrations (100−200 μM), the extent of activation was ~2.8 times that of the control (Figure 1A). According to our hypothesis (see model a in Figure 8), this suggests that DP15 interfered with the interdomain interaction between the 4820−4841 region (L_{6-7}, Figure 8) and its putative mating domain and activated the RyR channel. Importantly, a point mutation in DP15 mimicking the L4837V MH mutation (*10*, *11*) completely abolished the channel activating function of DP15 of [^{3}H]-ryanodine binding activity, although at higher concentrations (>100 μM), DP15mut began to exhibit slight activation. Similarly, another MH mutation, L4823P (*8*, *9*), almost completely abolished the channel activation function of DP15 over a range of low peptide concentrations (≤50 μM), but in this case, higher concentrations of the peptide produced significant activation (Figure 1A). The loss of the activation effect of DP15 caused by the mutation implies the loss of the ability to interfere with the stabilizing interdomain interaction. This suggests that the L4823P or L4837V mutation in the in vivo 4820−4841 region destabilizes the physiological interdomain interaction, leading to the abnormal channel activation seen in MH RyR1. At 0.1 μM Ca^{2+}, DP15 exhibited rather complex concentration-dependent effects on [^{3}H]ryanodine binding activity (Figure 1B). In a lower concentration range (10−50 μM), DP15 produced small but significant inhibition, and at concentrations higher than 100 μM, it produced activation. The L4837V MH mutation introduced into DP15 abolished both inhibitory and activation effects, although at the highest concentrations that were tested (200 and 300 μM) DP15mut produced a small activation.

In the experiment shown in Figure 2, we carried out [^{3}H]-ryanodine binding assays at various Ca^{2+} concentrations, in the presence or absence of 100 μM DP15. As shown, DP15 has dual Ca^{2+} concentration-dependent effects. Namely, the peptide inhibits RyR1 at subthreshold Ca^{2+} concentrations (≤0.2−0.3 μM) and activates at above-threshold Ca^{2+} concentrations (≥0.3 μM). Interestingly, the dual Ca^{2+} concentration dependence of channel inhibition and activation by DP15 is the complete opposite of the Ca^{2+} concentration dependence pattern of CaM regulation of RyR1, i.e., channel activation by CaM at low Ca^{2+} concentrations and inhibition at high Ca^{2+} concentrations (*17*−*19*).

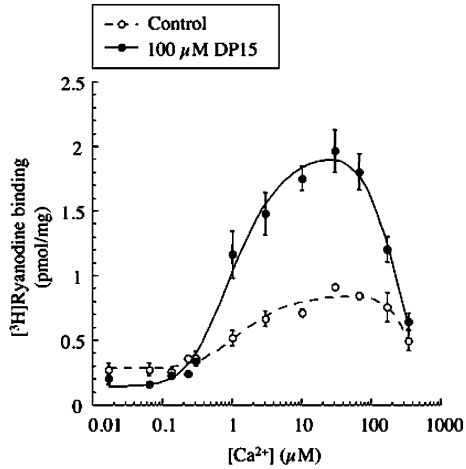

FIGURE 2: Ca^{2+} concentration dependence of binding of [^{3}H]-ryanodine to RyR1 in the absence and presence of DP15. [^{3}H]-Ryanodine binding assays were performed in the absence (control) or presence of 100 μM DP15 at various Ca^{2+} concentrations. At low Ca^{2+} concentrations (~0.3 μM), DP15 inhibited binding of [^{3}H]ryanodine to RyR1, while at higher Ca^{2+} concentrations (0.5−10 μM), DP15 activated. Beyond 10 μM Ca^{2+}, DP15 activity was reduced. $n = 4-9$ for control and 100 μM DP15.

Table 1: Domain Peptides Used in This Study

Domain peptide	Amino acid sequence
DP15	^{4820}VKTLRTILSSVTHNGKQLVMTV^{4841}
DP15mut(L4823P)	VKT**P**RTILSSVTHNGKQLVMTV
DP15mut(L4837V)	VKTLRTILSSVTHNGKQ**V**VMTV
DPc15	^{4752}FKTLRTILSSVTHNGKQLVLTV^{4773}
DPc15mut(H4764P)	FKTLRTILSSVT**P**NGKQLVLTV
DP17	^{4114}CSEADENEMINFEEFANRFQEPARDIGFN^{4142}
DP17mut(R4137S)	CSEADENEMINFEEFANRFQEPA**S**DIGFN

The cytoplasmic TM6−TM7 loop (L_{6-7}) of the cardiac RyR2 channel domain has a similar primary structure (cf. Table 1). This suggests that a similar mechanism operates also in cardiac channel regulation. We examined the effect of the cardiac counterpart of DP15, DPc15 (Table 1), on the

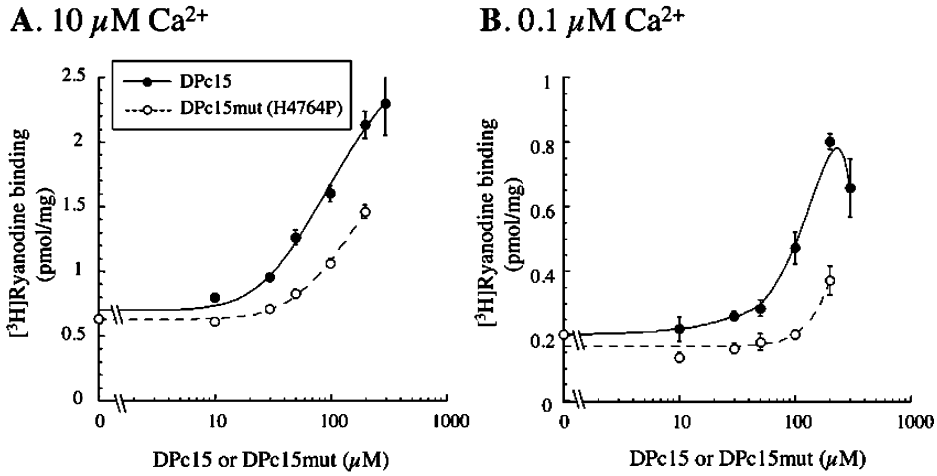

FIGURE 3: Concentration dependence of DPc15 and DPc15mut on binding of [^{3}H]ryanodine to RyR1. (A) Rabbit skeletal SR (0.5 mg/mL) was incubated with 10 nM [^{3}H]ryanodine in a solution of 0.15 M KCl, 20 mM MOPS (pH 7.2), 2 mM DTT, and various concentrations of DPc15 (●) and DPc15mut (H4764P) (○) at 10 μM Ca^{2+}. $n = 3-9$ for DPc15, and $n = 3$ for DPc15mut. (B) Similar experiments were performed at 0.1 μM Ca^{2+}. $n = 3-9$ for DPc15, and $n = 3$ for DPc15mut.

[^{3}H]ryanodine binding activity of RyR1 at 10 μM Ca^{2+} (Figure 3A) and 0.1 μM Ca^{2+} (Figure 3B). As shown, DPc15 produced significant activation of RyR1 at both 0.1 and 10 μM Ca^{2+}. Importantly, the H4764P CPVT mutation (*13*) in DPc15 resulted in a considerable attenuation of the activating function that would have been present in wild-type DPc15, although the extent of inhibition was significantly smaller than those for the skeletal muscle-type mutations introduced into DP15.

Fluorescence Labeling of the DP15 Binding Domain. Figure 4 depicts the results of our attempt to identify the region of the RyR1 to which DP15 binding takes place. We carried out photoaffinity cross-linking of fluorescently labeled DP15 to RyR1. DP15 was labeled with a fluorescent probe Alexa Fluor 680 and a photoaffinity cross-linking agent APG (see Experimental Procedures), and after incubation of the Alexa Fluor 680−DP15−APG conjugate at 10 μM Ca^{2+} for 1 min in the dark, the mixture of the peptide complex with the SR was photolyzed. The photoaffinity labeled SR was subjected to gel analysis. As shown, ~35% of the total fluorescence intensity incorporated into the SR proteins was associated with the RyR band. Since the content of RyR is ~4.3% of the total SR proteins (as determined by densitometry of the Coomassie blue-stained bands), almost exclusive fluorescent labeling has taken place in the RyR moiety of the SR in terms of specific incorporation of a fluorescent marker. Digestion with calpain II and increasing concentrations of trypsin produced various extents of cleavage of the RyR polypeptide chain, and we identified the regions of RyR from which the fluorescent fragments originate using polyclonal antibodies directed to the 3614−3643 (anti-CaMBP Ab) and 4114−4142 (anti-DP17 Ab) regions. As summarized in Figure 4B, the fluorescent label was localized first in a 400 kDa calpain fragment; after extensive digestion (4000:1), it was localized in a 120 kDa tryptic fragment which was stained with both antibodies. Upon further digestion (1000:1), the fluorescence intensity was primarily in a 96 kDa fragment which was stained with anti-DP17 Ab, but not with anti-CaMBP Ab. These results indicate that binding of DP15 to the 96 kDa region of RyR1 containing the 4114−4142 region took place (D_{96k}, Figure 8).

Anti-DP15 Antibody and DP17 (a peptide corresponding to the 4114−4142 region) Also Activate RyR1. The finding that DP15 binds to the 4114−4142 region suggests that there is an interdomain interaction between L_{6-7} (the cytoplasmic loop adjacent to the channel pore) and D_{96k} [the 96 kDa region containing CaM-like/Ca^{2+} regulatory domain (*19*)], as schematically illustrated in Figure 8. The fact that DP15 activates the RyR1 channel in a Ca^{2+}-dependent manner (Figures 1 and 2) suggests that at near or above-threshold Ca^{2+} concentrations the binding of DP15 to the D_{96k} in competition with the in vivo interaction of L_{6-7} with D_{96k} interferes with the $L_{6-7}-D_{96k}$ interdomain interaction and unzips these interacting domains to activate the channel (cf. scheme a of Figure 8). If the observed activation is due to interference with a domain−domain interaction rather than a direct effect of peptide binding, then we would expect that an antibody directed to DP15 should produce activation effects comparable with that produced by DP15. As shown in Figure 5, anti-DP15 Ab (200 μg/mL) produced a significant activation of [^{3}H]ryanodine binding activity at both 0.1 and 10 μM Ca^{2+}. Preimmune sera did not show any significant activation at the same concentration (data not shown). The results suggest that the antibody directed to the M6−M7 loop (L_{6-7}) interfered with the postulated $D_{96k}-L_{6-7}$ interaction, resulting in channel activation.

Figure 6 shows the concentration-dependent effect of another domain peptide, DP17 (matching the 4114−4142 region of region 3 of RyR1), on [^{3}H]ryanodine binding activity at 10 μM Ca^{2+} (A) and 0.1 μM Ca^{2+} (B). At 10 μM Ca^{2+}, DP17 activated [^{3}H]ryanodine binding activity, yielding a concentration-dependent pattern similar to that of DP15 and DPc15, although the extent of activation was much smaller compared to those of the DP15 peptides. An MH mutation (R4137S) introduced into DP17 produced an ~50% reduction of the activating function of wild-type DP17. At 0.1 μM Ca^{2+}, DP17 produced no appreciable effect on the [^{3}H]ryanodine binding activity over the range of peptide concentrations that were tested. Figure 7 shows the Ca^{2+} concentration dependence of [^{3}H]ryanodine binding activity in the absence (control) and presence of 100 μM DP17. The data show that the activation of DP17 occurs with no

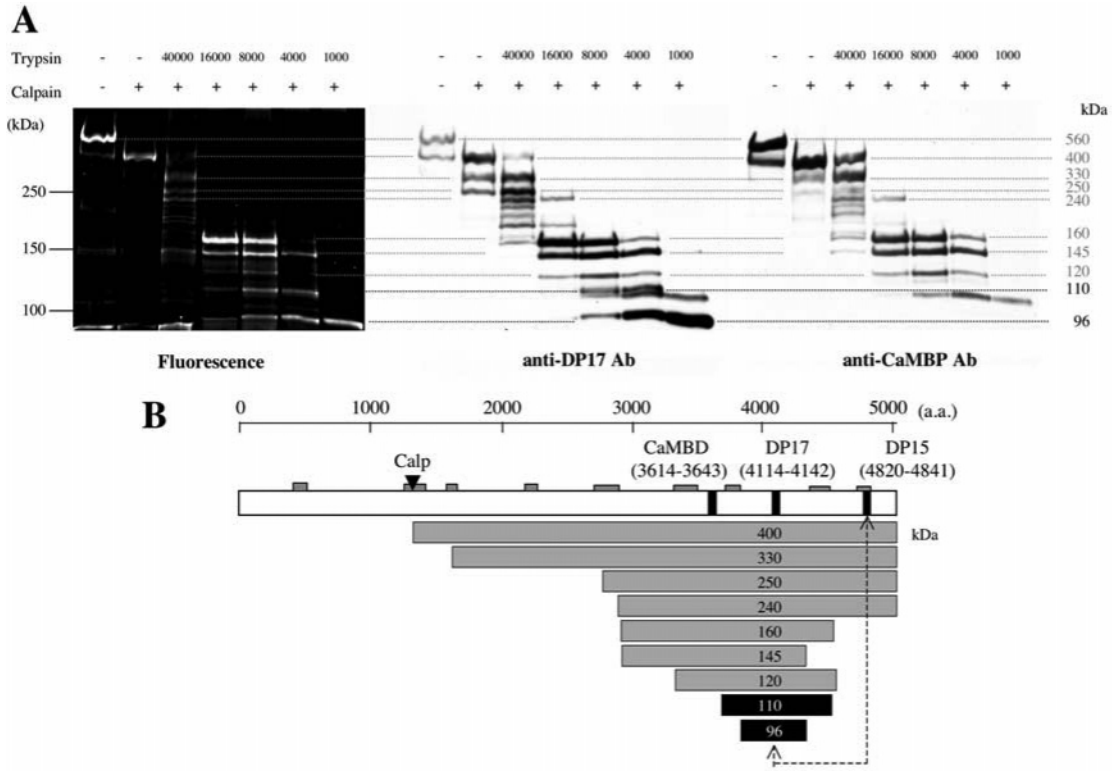

FIGURE 4: Site-specific fluorescence labeling of the DP15 binding domain of RyR1. (A) Fluorogram and Western blot with anti-DP17 antibody (anti-DP17 Ab) and anti-CaMBP antibody (anti-CaMBP Ab). The Alexa Fluor 680−DP15−APG conjugate produced a specific labeling of RyR1 in SR. The Alexa 680 labeling with DP15 is localized in a 96 kDa fragment of RyR after calpain and trypsin digestion, which was detected with anti-DP17 antibody (anti-DP17 Ab) but not with anti-CaMBP antibody (anti-CaMBP Ab). (B) Digestion map of RyR1 with calpain and trypsin. The map was modified from the figure of Chen et al. (*29*). Calpain-sensitive and protease-sensitive regions (*29*, *30*) are identified with a black inverted triangle and a gray box, respectively. The Alexa 680 labeling with DP15 was detected in the following fragments: 400, 330, 250, 240, 160, 145, 120, 110, and 96 kDa. The 110 and 96 kDa fragments (black boxes) were stained with anti-DP17 antibody, not with anti-CaMBP antibody. The data show that the DP15 binding domain is in the 96 kDa fragment that includes the DP17 region.

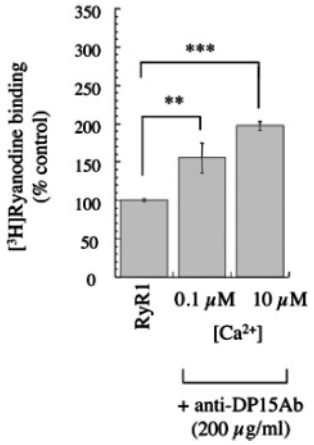

FIGURE 5: Anti-DP15 antibody enhances binding of [^{3}H]ryanodine to RyR1. Rabbit skeletal SR (0.5 mg/mL) was incubated with 10 nM [^{3}H]ryanodine in a solution of 0.15 M KCl and 20 mM MOPS (pH 7.2) at two different Ca^{2+} concentrations (0.1 and 10 μM) in the absence (RyR1) and presence of 200 μg/mL anti-DP15 antibody. The solution was incubated at 22 °C overnight. Three asterisks indicate a P of <0.0001 and two asterisks a P of <0.01 vs RyR1. $n = 3-7$.

appreciable change in the overall Ca^{2+} concentration dependence pattern. The results suggest that DP17, which represents a part of D_{96k} (the partner domain of L_{6-7}), also interferes with the $D_{96k}-L_{6-7}$ interaction, again causing channel activation.

DISCUSSION

A considerable number of mutations and deletions linked with MH and CCD have been reported in region 3 encompassing residues 3916−4973 of RyR1 (*20*, *21*). Region 3 includes the majority of the I domain (residues 3760−4679 of RyR1 corresponding to residues 3722−4610 of RyR2), which seems to be critical for the interaction between the cytoplasmic regulatory domain of RyR1 and the transmembrane channel domain (*5*). Also included in region 3 is a segment (residues 4064−4210) that resembles the structure of CaM (CaM-like domain, CaMLD). According to recent work by Hamilton and her colleagues (*19*), an expressed peptide corresponding to this segment shows several CaM-like properties. Importantly, CaMLD contains EF-hand-like sequences that are probably involved in Ca^{2+}-dependent regulation (*22*, *23*).

One of the important findings in this study is the fact that DP15 binds with a 96 kDa segment containing the CaMLD region, as shown by photoaffinity cross-linking of a fluorescent DP15 and Western blot of the fluorescence-labeled tryptic fragment with a site-specific antibody directed to the 4114−4142 region. This suggests that there is an interaction between the TM6−TM7 loop (L_{6-7}, Figure 8) and the 96 kDa region containing CaMLD (D_{96k}, Figure 8). DP15 was found to produce significant activation of [^{3}H]ryanodine binding at above-threshold Ca^{2+} concentrations (≥ 0.3 μM), although it produced rather complex effects at a low Ca^{2+}

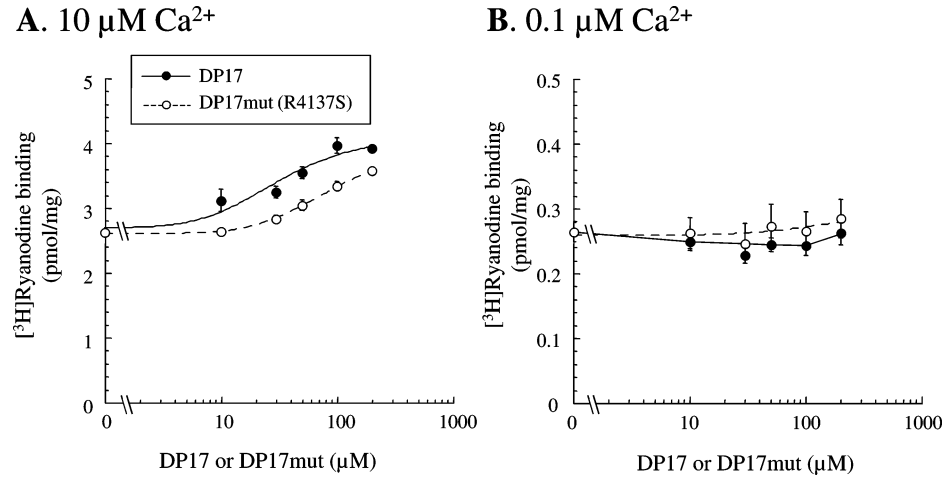

FIGURE 6: Concentration dependence of DP17 and DP17mut on binding of [^{3}H]ryanodine to RyR1. (A) Rabbit skeletal SR (0.5 mg/mL) was incubated with 10 nM [^{3}H]ryanodine in a solution of 0.15 M KCl, 20 mM MOPS (pH 7.2), and various concentrations of DP17 (●) and DP17mut (R4137S) (○) at 10 μM Ca^{2+}. $n = 3-6$ for DP17, and $n = 3$ for DP17mut. (B) Similar experiments were performed at 0.1 μM Ca^{2+}. $n = 3-6$ for DP17, and $n = 3$ for DP17mut.

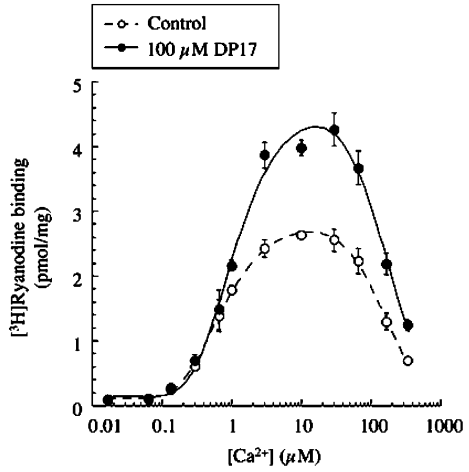

FIGURE 7: Ca^{2+} concentration dependence of binding of [^{3}H]-ryanodine to RyR1 in the absence and presence of DP17. [^{3}H]-Ryanodine binding assays were performed in the absence (control) or presence of 100 μM DP17 at various Ca^{2+} concentrations. $n = 3-6$ for control and 100 μM DP17.

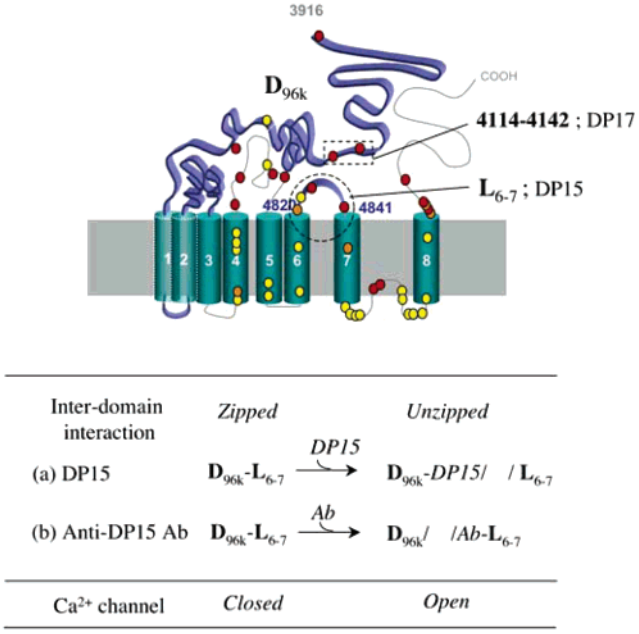

FIGURE 8: Schematic model of the interdomain interaction in region 3 of RyR1. The schematic model of region 3 on RyR1 (residues 3916−5037) was based on the topology of the transmembrane by Du et al. (*15*, *16*). According to Du's model, there are eight transmembrane (TM) segments. The MH/CCD mutation sites were based on published data (*8*−*11*, *13*, *31*−*43*). The MH (red circles) or MH/CCD (orange circles) mutation sites are located in the cytoplasmic region or channel pore region (between TM7 and TM8), while CCD (yellow circles) mutation sites are mainly localized in the helices of transmembrane regions. The interdomain hypothesis we tested in this study is summarized in the table at the bottom. In the nonactivated state, the 96 kDa domain (D_{96k}) and the TM6−TM7 loop (L_{6-7}) are tightly bound with each other (zipped, D_{96k}−L_{6-7}), stabilizing the closed state of the channel. In reaction a, DP15 binds with its mating domain (D_{96k}), in competition with L_{6-7}, causing partial domain unzipping (D_{96k}-DP15/ /L_{6-7}) and channel activation, mimicking the effect produced by the mutation in L_{6-7}. In reaction b, antibody directed to L_{6-7} (anti-DP15 Ab) also causes domain unzipping and channel activation by interfering with the D_{96k}−L_{6-7} interaction.

concentration (0.1 μM). An antibody directed to DP15 produced significant activation of [^{3}H]ryanodine binding activity at both low and high Ca^{2+} concentrations. Furthermore, the cardiac counterpart of DP15, i.e., DPc15, produced significant activation of [^{3}H]ryanodine binding at both low and high Ca^{2+} concentrations. According to our domain peptide probe hypothesis, these results suggest that the binding of DP15 or DPc15 with CaMLD containing the 96 kDa region (D_{96k}, Figure 8, scheme a) or the binding of the anti-DP15 antibody with the cytoplasmic TM6−TM7 loop (L_{6-7}, Figure 8, scheme b) interfered with the interdomain interaction between D_{96k} and L_{6-7}, resulting in "domain unzipping" and channel activation. This is basically the same mechanism as that previously described for channel activation induced by the interference of the interdomain interaction between region 1 and region 2 by the domain switch-directed peptides, such as DP4 (*1*−*4*). However, there is one unique feature characteristic of DP15. That is, under specific conditions (lower concentrations of the peptide, at subthreshold Ca^{2+} concentrations), DP15 produced weak but significant inhibition (Figures 1 and 2). Higher concentrations of DP15 produce activation even at 0.1 μM Ca^{2+} (cf. Figure 1), and according to our preliminary data, with an increase in the concentration of KCl in the assay solution

from 0.15 to 1.0 M, DP15 (100 μM) exhibited significant activation (130% control) even at 0.1 μM Ca^{2+} (data not shown). We propose that DP15 probes two events: (a) interference of the channel-stabilizing interdomain interaction that leads to channel activation and (b) binding of DP15 to the putative "inhibitory site(s)" within D_{96k} that leads to channel inhibition. Under the conditions that favor channel activation such as higher concentrations of Ca^{2+} and KCl, the effect of DP15 on event (a) is manifested predominantly.

These data which show that anti-DP15 antibody, which binds with L_{6-7} but not with D_{96k}, produced activation at both low and high Ca^{2+} concentrations are consistent with the view that interference of the interdomain interaction, rather than the peptide binding a specific activation site(s), is the underlying mechanism for channel activation. In further support of this view, another domain peptide, DP17, corresponding to a portion of D_{96k} also produced channel activation.

Figure 8 illustrates our tentative topographical arrangement of the CaMLD-containing 96 kDa region relative to the transmembrane helices (cf. refs *15* and *16*). When we plot the reported MH mutations (red circle) and CCD mutations (yellow circle) in the map, it reveals an interesting feature in the distribution of the two types of mutations. As seen, most (if not all) of the MH mutations producing a relatively mild phenotype (*24*) are localized in the cytoplasmic area, while most CCD mutations producing more severe phenotypes (*25*, *26*) are located at the luminal side of the SR membrane, particularly in the putative channel pore region (*27*). It is worth noting that some of the MH mutations in region 3, as tested in a homologous expression system, exhibit a phenotype similar to those in regions 1 and 2 (*28*). As shown in the study presented here, single mutations made in DP15, mimicking the L4823P or L4837V MH mutations, produced a severe impact on the channel activating function of wild-type DP15. This suggests that MH mutation in the TM6−TM7 loop (L_{6-7}) weakened the domain−domain interaction and produced hyperactivation effects on the channel (a common phenotype of MH mutations), again the same mechanism previously described for the effect of mutations in regions 1 and 2 (*1*−*4*). Similarly, MH mutation in the D_{96k} domain, such as R4137S introduced into DP17, weakens the interdomain interaction, leading to channel activation. Interestingly, cardiac-type DP15, i.e., DPc15, led to a significant activation of RyR1, and a CPVT (*12*) mutation introduced into DPc15 produced a severe impact on the activating function of the peptide, as shown in this study. Thus, it may not be unreasonable to assume that the TM6−TM7 loop (L_{6-7}) is involved in a domain−domain interaction and channel regulation also in RyR2.

In conclusion, application of a peptide probe matching the cytoplasmic TM6−TM7 loop (residues 4820−4841) to region 3 of RyR1 (DP15) has revealed an interdomain interaction between the TM6−TM7 loop and the 96 kDa segment containing CaM-like domain (but not including the CaM-binding domain). Significant activation of RyR1 channels by either DP15 or an antibody directed to this peptide (i.e., TM6−TM7 loop) suggests that tighter domain−domain interaction stabilizes the closed state of the channel, and weakened interaction (unzipping) activates the channel. MH or CPVT mutation occurring in the loop, and perhaps mutation in the 96 kDa domain as well, weakens the domain−domain interaction and destabilizes the channel.

ACKNOWLEDGMENT

We thank Dr. Renne C. Lu, Dr. Paul Leavis, David Schrier, and Elizabeth Gowell for synthesis and purification of the peptides. We also thank Dr. Jaya P. Gangopadhyay for purification of the anti-CaMBP and DP17 antibodies.

REFERENCES

1. Yamamoto, T., El-Hayek, R., and Ikemoto, N. (2000) Postulated role of interdomain interaction within the ryanodine receptor in Ca^{2+} channel regulation, *J. Biol. Chem. 275*, 11618−11625.
2. Yamamoto, T., and Ikemoto, N. (2002) Spectroscopic monitoring of local conformational changes during the intramolecular domain-domain interaction of the ryanodine receptor, *Biochemistry 41*, 1492−1501.
3. Ikemoto, N., and Yamamoto, T. (2002) Regulation of calcium release by interdomain interaction within ryanodine receptors, *Front. Biosci. 7*, d671−d683.
4. Kobayashi, S., Yamamoto, T., Parness, J., and Ikemoto, N. (2004) Antibody probe study of Ca^{2+} channel regulation by interdomain interaction within the ryanodine receptor, *Biochem. J. 380*, 561−569.
5. George, C. H., Jundi, H., Thomas, N. L., Scoote, M., Walters, N., Williams, A. J., and Lai, F. A. (2004) Ryanodine receptor regulation by intramolecular interaction between cytoplasmic and transmembrane domains, *Mol. Biol. Cell 15*, 2627−2638.
6. Gilman, C. P., Galvan, D. L., Cheng, Q., and Hamilton, S. L. (2006) A Predicted Ca^{2+} Binding Sequence (amino acids 4062−4210) of RyR1 Interacts with Its Carboxyl-Terminal Region, 50th Biophysical Society Annual Meeting, Feb 18−22, 2006, Salt Lake City, UT, Poster 1885.
7. Ikemoto, N., Kim, D. H., and Antoniu, B. (1988) Measurement of calcium release in isolated membrane systems: Coupling between the transverse tubule and sarcoplasmic reticulum, *Methods Enzymol. 157*, 469−480.
8. Sei, Y., Sambuughin, N. N., Davis, E. J., Sachs, D., Cuenca, P. B., Brandom, B. W., Tautz, T., Rosenberg, H., Nelson, T. E., and Muldoon, S. M. (2004) Malignant hyperthermia in North America: Genetic screening of the three hot spots in the type I ryanodine receptor gene, *Anesthesiology 101*, 824−830.
9. Shepherd, S., Ellis, F., Halsall, J., Hopkins, P., and Robinson, R. (2004) RYR1 mutations in UK central core disease patients: More than just the C-terminal transmembrane region of the RYR1 gene, *J. Med. Genet. 41*, e33.
10. Oyamada, H., Oguchi, K., Saitoh, N., Yamazawa, T., Hirose, K., Kawana, Y., Wakatsuki, K., Tagami, M., Hanaoka, K., Endo, M., and Iino, M. (2002) Novel mutations in C-terminal channel region of the ryanodine receptor in malignant hyperthermia patients, *Jpn. J. Pharmacol. 88*, 159−166.
11. Ibarra, M. C., Wu, S., Murayama, K., Minami, N., Ichihara, Y., Kikuchi, H., Noguchi, S., Hayashi, Y. K., Ochiai, R., and Nishino, I. (2006) Malignant hyperthermia in Japan: Mutation screening of the entire ryanodine receptor type 1 gene coding region by direct sequencing, *Anesthesiology 104*, 1146−1154.
12. Postma, A. V., Denjoy, I., Kamblock, J., Alders, M., Lupoglazoff, J. M., Vaksmann, G., Dubosq-Bidot, L., Sebillon, P., Mannens, M. M., Guicheney, P., and Wilde, A. A. (2005) Catecholaminergic polymorphic ventricular tachycardia: RYR2 mutations, bradycardia, and follow up of the patients, *J. Med. Genet. 42*, 863−870.
13. Galli, L., Orrico, A., Cozzolino, S., Pietrini, V., Tegazzin, V., and Sorrentino, V. (2002) Mutations in the RYR1 gene in Italian patients at risk for malignant hyperthermia: Evidence for a cluster of novel mutations in the C-terminal region, *Cell Calcium 32*, 143−151.
14. Laemmli, U. K., and Favre, M. (1973) Maturation of the head of bacteriophage T4. I DNA packaging events, *J. Mol. Biol. 80*, 575−599.
15. Du, G. G., Sandhu, B., Khanna, V. K., Guo, X. H., and MacLennan, D. H. (2002) Topology of the Ca^{2+} release channel of skeletal muscle sarcoplasmic reticulum (RyR1), *Proc. Natl. Acad. Sci. U.S.A. 99*, 16725−16730.

16. Du, G. G., and MacLennan, D. H. (2005) in *Ryanodine Receptors: Structure, Function and Dysfunction in Clinical Disease* (Wehrens, X. H. T., and Marks, A. R., Eds.) pp 9−23, Springer, New York.
17. Tang, W., Sencer, S., and Hamilton, S. L. (2002) Calmodulin modulation of proteins involved in excitation-contraction coupling, *Front. Biosci. 7*, d1583−d1589.
18. Gangopadhyay, J. P., Grabarek, Z., and Ikemoto, N. (2004) Fluorescence probe study of Ca^{2+}-dependent interactions of calmodulin with calmodulin-binding peptides of the ryanodine receptor, *Biochem. Biophys. Res. Commun. 323*, 760−768.
19. Xiong, L., Zhang, J. Z., He, R., and Hamilton, S. L. (2006) A Ca^{2+}-binding domain in RyR1 that interacts with the calmodulin binding site and modulates channel activity, *Biophys. J. 90*, 173−182.
20. Lyfenko, A. D., Goonasekera, S. A., and Dirksen, R. T. (2004) Dynamic alterations in myoplasmic Ca^{2+} in malignant hyperthermia and central core disease, *Biochem. Biophys. Res. Commun. 322*, 1256−1266.
21. Avila, G. (2005) Intracellular Ca^{2+} dynamics in malignant hyperthermia and central core disease: Established concepts, new cellular mechanisms involved, *Cell Calcium 37*, 121−127.
22. Zorzato, F., Fujii, J., Otsu, K., Phillips, M., Green, N. M., Lai, F. A., Meissner, G., and MacLennan, D. H. (1990) Molecular cloning of cDNA encoding human and rabbit forms of the Ca^{2+} release channel (ryanodine receptor) of skeletal muscle sarcoplasmic reticulum, *J. Biol. Chem. 265*, 2244−2256.
23. Fessenden, J. D., Feng, W., Pessah, I. N., and Allen, P. D. (2004) Mutational analysis of putative calcium binding motifs within the skeletal ryanodine receptor isoform, RyR1, *J. Biol. Chem. 279*, 53028−53035.
24. Treves, S., Anderson, A. A., Ducreux, S., Diver, A., Belunven, C., Grasso, C., Paesante, S., and Zorzato, F. (2005) Ryanodine receptor 1 mutations, dysregulation of calcium homeostasis and neuromuscular disorders. *Neuromuscular Disord. 15*, 577−587.
25. Lynch, P. J., Tong, J., Lehane, M., Mallet, A., Giblin, L., Heffron, J. J., Vaughan, P., Zafra, G., MacLennan, D. H., and McCarthy, T. V. (1999) A mutation in the transmembrane/luminal domain of the ryanodine receptor is associated with abnormal Ca^{2+} release channel function and severe central core disease, *Proc. Natl. Acad. Sci. U.S.A. 96*, 4164−4169.
26. Avila, G., and Dirksen, R. T. (2001) Functional effects of central core disease mutations in the cytoplasmic region of the skeletal muscle ryanodine receptor, *J. Gen. Physiol. 118*, 277−290.
27. Avila, G., O'Connell, K. M., and Dirksen, R. T. (2003) The pore region of the skeletal muscle ryanodine receptor is a primary locus for excitation-contraction uncoupling in central core disease, *J. Gen. Physiol. 121*, 277−286.
28. Yang, T., Ta, T. A., Pessah, I. N., and Allen, P. D. (2003) Functional defects in six ryanodine receptor isoform-1 (RyR1) mutations associated with malignant hyperthermia and their impact on skeletal excitation-contraction coupling, *J. Biol. Chem. 278*, 25722−25730.
29. Chen, S. R., Airey, J. A., and MacLennan, D. H. (1993) Positioning of major tryptic fragments in the Ca^{2+} release channel (ryanodine receptor) resulting from partial digestion of rabbit skeletal muscle sarcoplasmic reticulum, *J. Biol. Chem. 268*, 22642−22649.
30. Marks, A. R., Fleischer, S., and Tempst, P. (1990) Surface topography analysis of the ryanodine receptor/junctional channel complex based on proteolysis sensitivity mapping, *J. Biol. Chem. 265*, 13143−13149.
31. Monnier, N., Krivosic-Horber, R., Payen, J. F., Kozak-Ribbens, G., Nivoche, Y., Adnet, P., Reyford, H., and Lunardi, J. (2002) Presence of two different genetic traits in malignant hyperthermia families: Implication for genetic analysis, diagnosis, and incidence of malignant hyperthermia susceptibility, *Anesthesiology 97*, 1067−1074.
32. Sambuughin, N., Holley, H., Muldoon, S., Brandom, B. W., de Bantel, A. M., Tobin, J. R., Nelson, T. E., and Goldfarb, L. G. (2005) Screening of the entire ryanodine receptor type 1 coding region for sequence variants associated with malignant hyperthermia susceptibility in the North American population, *Anesthesiology 102*, 515−521.
33. Monnier, N., Romero, N. B., Lerale, J., Landrieu, P., Nivoche, Y., Fardeau, M., and Lunardi, J. (2001) Familial and sporadic forms of central core disease are associated with mutations in the C-terminal domain of the skeletal muscle ryanodine receptor, *Hum. Mol. Genet. 10*, 2581−2592.
34. Scacheri, P. C., Hoffman, E. P., Fratkin, J. D., Semino-Mora, C., Senchak, A., Davis, M. R., Laing, N. G., Vedanarayanan, V., and Subramony, S. H. (2000) A novel ryanodine receptor gene mutation causing both cores and rods in congenital myopathy, *Neurology 55*, 1689−1696.
35. Davis, M. R., Haan, E., Jungbluth, H., Sewry, C., North, K., Muntoni, F., Kuntzer, T., Lamont, P., Bankier, A., Tomlinson, P., Sanchez, A., Walsh, P., Nagarajan, L., Oley, C., Colley, A., Gedeon, A., Quinlivan, R., Dixon, J., James, D., Muller, C. R., and Laing, N. G. (2003) Principal mutation hotspot for central core disease and related myopathies in the C-terminal transmembrane region of the RYR1 gene, *Neuromuscular Disord. 13*, 151−157.
36. Romero, N. B., Monnier, N., Viollet, L., Cortey, A., Chevallay, M., Leroy, J. P., Lunardi, J., and Fardeau, M. (2003) Dominant and recessive central core disease associated with RYR1 mutations and fetal akinesia, *Brain 126*, 2341−2349.
37. Monnier, N., Kozak-Ribbens, G., Krivosic-Horber, R., Nivoche, Y., Qi, D., Kraev, N., Loke, J., Sharma, P., Tegazzin, V., Figarella-Branger, D., Romero, N., Mezin, P., Bendahan, D., Payen, J. F., Depret, T., Maclennan, D. H., and Lunardi, J. (2005) Correlations between genotype and pharmacological, histological, functional, and clinical phenotypes in malignant hyperthermia susceptibility, *Hum. Mutat. 26*, 413−425.
38. Brown, R. L., Pollock, A. N., Couchman, K. G., Hodges, M., Hutchinson, D. O., Waaka, R., Lynch, P., McCarthy, T. V., and Stowell, K. M. (2000) A novel ryanodine receptor mutation and genotype-phenotype correlation in a large malignant hyperthermia New Zealand Maori pedigree, *Hum. Mol. Genet. 9*, 1515−1524.
39. Jungbluth, H., Muller, C. R., Halliger-Keller, B., Brockington, M., Brown, S. C., Feng, L., Chattopadhyay, A., Mercuri, E., Manzur, A. Y., Ferreiro, A., Laing, N. G., Davis, M. R., Roper, H. P., Dubowitz, V., Bydder, G., Sewry, C. A., and Muntoni, F. (2002) Autosomal recessive inheritance of RYR1 mutations in a congenital myopathy with cores, *Neurology 59*, 284−287.
40. Tilgen, N., Zorzato, F., Halliger-Keller, B., Muntoni, F., Sewry, C., Palmucci, L. M., Schneider, C., Hauser, E., Lehmann-Horn, F., Muller, C. R., and Treves, S. (2001) Identification of four novel mutations in the C-terminal membrane spanning domain of the ryanodine receptor 1: Association with central core disease and alteration of calcium homeostasis, *Hum. Mol. Genet. 10*, 2879−2887.
41. Zorzato, F., Yamaguchi, N., Xu, L., Meissner, G., Muller, C. R., Pouliquin, P., Muntoni, F., Sewry, C., Girard, T., and Treves, S. (2003) Clinical and functional effects of a deletion in a COOH-terminal lumenal loop of the skeletal muscle ryanodine receptor, *Hum. Mol. Genet. 12*, 379−388.
42. Lynch, P. J., Krivosic-Horber, R., Reyford, H., Monnier, N., Quane, K., Adnet, P., Haudecoeur, G., Krivosic, I., McCarthy, T., and Lunardi, J. (1997) Identification of heterozygous and homozygous individuals with the novel RYR1 mutation Cys35Arg in a large kindred, *Anesthesiology 86*, 620−626.
43. Ducreux, S., Zorzato, F., Muller, C., Sewry, C., Muntoni, F., Quinlivan, R., Restagno, G., Girard, T., and Treves, S. (2004) Effect of ryanodine receptor mutations on interleukin-6 release and intracellular calcium homeostasis in human myotubes from malignant hyperthermia-susceptible individuals and patients affected by central core disease, *J. Biol. Chem. 279*, 43838−43846.

BI061557F